PHYSICAL REVIEW A VOLUME 14, NUMBER 3 SEPTEMBER 1976

Moment-theory investigations of photoabsorption and dispersion profiles in atoms and ions

P. W. Langhoff
Department of Chemistry, Indiana University, Bloomington, Indiana 47401,
Department of Chemistry, Stanford University, Stanford, California 94305,
Joint Institute for Laboratory Astrophysics, National Bureau of Standards and University of Colorado, Boulder, Colorado 80309,

C. T. Corcoran and J. S. Sims
Department of Chemistry, Indiana University, Bloomington, Indiana 47401

F. Weinhold and R. M. Glover
Department of Chemistry, Stanford University, Stanford, California 94305
(Received 11 March 1976)

Moment-theory methods for the construction of photoabsorption and dispersion profiles from associated dipole spectral moments are described and applied to simple atoms and ions. A previously devised (Stieltjes) moment approach, which provides convergent histogram approximations to absorption and dispersion profiles, is refined and extended to the use of arbitrarily large numbers of spectral moments, and an improved (Tchebycheff) moment approach is introduced which gives profiles that are continuous in the photoionization region and exhibit the δ-function-like behavior associated with discrete transitions at the appropriate frequencies. Recurrence relations for the polynomials orthogonal and quasiorthogonal with respect to the distributions are employed in solving the necessary moment problems involving large numbers of spectral moments. The methods are applied in illustrative calculations of absorption and dispersion profiles in one- and two-electron atoms and ions. In the case of one-electron atomic systems the necessary polynomial recurrence coefficients are obtained in closed form from the known spectral moments, allowing the construction of distributions which reproduce the known profiles with high accuracy, employing as many as 100 spectral moments. Variational calculations using large basis sets of square-integrable functions, including the special functions required to satisfy sum rules, provide accurate spectral moments for atomic helium and the negative hydrogen ion. A simple moment-extension procedure is devised to interpolate the associated recurrence coefficients to infinite order employing their known asymptotic values. The associated Stieltjes and Tchebycheff approximations to the absorption and dispersion profiles obtained in these cases are in excellent agreement with available measurements and previous accurate calculations employing discrete and continuum wave functions.

I. INTRODUCTION

The photoabsorption and dispersion profiles of atoms and ions in the optical and uv portions of the spectrum have long been the focus of considerable theoretical and experimental investigation.[1] Only comparatively recently, however, have accurate measurements and calculations provided profiles in good mutual agreement for even the simplest atomic systems.[2] Although Schrödinger theory in the semiclassical approximation furnishes the basis for theoretical investigations,[3] construction of the discrete and continuum eigenfunctions required in the customary expressions for absorption and dispersion cross-sections necessitates the introduction of additional approximations which are generally without *a priori* justification.[4]

Recently, techniques have been devised that can avoid additional approximations in semiclassical calculations of the interactions between radiation and matter.[5-7] One of these makes use of the classical theory of moments and conventional Ritz variational calculations appropriate for bound states to obtain accurate discrete and continuum absorption and dispersion profiles in atoms and ions.[6]

In the present paper the previously described (Stieltjes) moment approach,[8] which provides convergent histogram approximations to photoabsorption and dispersion profiles from a given set of spectral moments, is refined and extended to the use of arbitrarily large numbers of spectral moments. In addition, a complementary and improved (Tchebycheff) moment approach is described that provides convergent approximations to absorption and dispersion profiles which are continuous in the photoionization region and give the singular behavior associated with discrete transitions at the appropriate frequencies. The moment problems arising in the construction of the Stieltjes and Tchebycheff profiles are solved for arbitrarily large numbers of moments by constructing the orthogonal and quasiorthogonal polynomials associated with the correct distributions,[9] using stable algorithms to calculate the polynomial recurrence coefficients from spectral moments[10]

or variationally-determined pseudospectra.

The Stieltjes and Tchebycheff moment methods are applied in illustrative calculations of absorption and dispersion profiles in one- and two-electron atoms and ions. In the case of one-electron atoms and ions, the necessary polynomial recurrence coefficients are obtained in closed forms, affording the construction of Stieltjes and Tchebycheff profiles corresponding to the use of up to 100 spectral moments which are rapidly convergent to the correct known results. Large basis-set variational calculations, including the special functions necessary to satisfy dipole sum rules,[11] are used to construct $^1S_0^e$ ground states and $^1P_1^o$ pseudostates for atomic helium and the negative hydrogen ion, from which the necessary spectral moments are obtained. The associated polynomial recurrence coefficients are found to converge rapidly to asymptotic values determined by the known frequency thresholds for photoionization, allowing their extension to arbitrary order using appropriate analytic forms. Convergent Stieltjes and Tchebycheff photoabsorption and dispersion profiles in atomic helium and the negative hydrogen ion are thereby obtained which are in excellent agreement with available measurements and the most accurate previous calculations employing discrete and continuum wave functions.

The Stieltjes and Tchebycheff approaches to photoabsorption and dispersion profiles are described in Sec. II, and some computational aspects of the methods are clarified. Applications are given in Sec. III and concluding remarks in Sec. IV.

II. THEORY

In this section we describe the Stieltjes and Tchebycheff procedures for constructing convergent approximations to photoabsorption and dispersion profiles from appropriate spectral moments or variationally determined pseudospectra, and clarify some of the computational aspects of the development.

A. Photoabsorption and dispersion

The photoabsorption cross section $\sigma(\omega)$ and refractive index $n(\omega)$ of a dilute gas are given by the expressions[12,13]

$$\sigma(\omega) = (4\pi\omega/c)\,\mathrm{Im}\,\alpha(\omega)\ , \tag{1}$$

$$n(\omega) = 1 + 2\pi N_0\,\mathrm{Re}\,\alpha(\omega)\ , \tag{2}$$

where c is the speed of light, N_0 is the atomic-number density, and the complex polarizability $\alpha(z)$ is given by the familiar Riemann-Stieltjes integral[6]

$$\alpha(z) = \int_{\epsilon_1}^{\infty} \frac{df(\epsilon)}{\epsilon^2 - z^2}\ , \tag{3a}$$

where

$$\mathrm{Im}\,\alpha(\omega) = \frac{\pi\, df(\epsilon)/d\epsilon}{2\omega}\ , \tag{3b}$$

$$\mathrm{Re}\,\alpha(\omega) = P\int_{\epsilon_1}^{\infty} \frac{df(\epsilon)}{\epsilon^2 - \omega^2}\ . \tag{3c}$$

Here, the oscillator strength for transition into the interval ϵ to $\epsilon + d\epsilon$ is given by

$$df(\epsilon) = \left(\sum_{i=1}^{\infty} f_i\,\delta(\epsilon_i - \epsilon) + g(\epsilon)\right) d\epsilon\ , \tag{4}$$

where the discrete and continuum contributions have their customary meanings.[3] In the following, we shall make use of the spectral moments[14]

$$S(-k) = \int_{\epsilon_1}^{\infty} \epsilon^{-k}\, df(\epsilon), \quad k \geq 0\ , \tag{5}$$

which are necessary and sufficient for the evaluation of Eqs. (1)–(3).[5]

B. Stieltjes procedure

Following the Stieltjes approach, convergent approximations to the polarizability of Eq. (3) that are valid for all complex z, including the real axis, are obtained in the form[8]

$$\alpha(z) = \int_{\epsilon_1}^{\infty} \frac{df^{(n)}(\epsilon)}{\epsilon^2 - z^2} + R_n(z), \quad n = 1, 2, \ldots, \tag{6}$$

where the distribution function $f^{(n)}(\epsilon)$ is given by an n-term sum of Stieltjes step-function integrators, and the remainder $R_n(z)$ is of known sign along certain rays. The positions $\epsilon_i(n)$ and strengths $f_i(n)$ of the steps of $f^{(n)}(\epsilon)$, which provide the histogram representation[6,9]

$$f^{(n)}(\epsilon) = 0, \quad 0 < \epsilon < \epsilon_1(n)\ , \tag{7a}$$

$$f^{(n)}(\epsilon) = \sum_{i=1}^{j} f_i(n), \quad \epsilon_j(n) < \epsilon < \epsilon_{j+1}(n)\ , \tag{7b}$$

$$f^{(n)}(\epsilon) = \sum_{i=1}^{n} f_i(n) = S(0), \quad \epsilon_n(n) < \epsilon\ , \tag{7c}$$

that give upper and lower (Tchebycheff) bounds on $f(\epsilon)$ at the points $\epsilon_i(n)$, are determined uniquely from solution of the moment problem[5,6,9]

$$S(-k) = \sum_{i=1}^{n} \epsilon_i(n)^{-k} f_i(n), \quad k = 0, 1, \ldots, 2n-1\ . \tag{8}$$

In the analytic region of the polarizability $\alpha(z)$, it is sufficient to interpret $df^{(n)}(\epsilon)$ of the histogram of Eqs. (7) in the Dirac sense,

$$df^{(n)}(\epsilon) = \left(\sum_{i=1}^{n} f_i(n)\, \delta(\epsilon_i(n) - \epsilon) \right) d\epsilon \,, \tag{9}$$

in which case Eq. (6) becomes[5] in the analytic region

$$\alpha(z) = \sum_{i=1}^{n} \frac{f_i(n)}{\epsilon_i(n)^2 - z^2} + R_n(z) \,. \tag{10}$$

By contrast, on the real axis we write

$$df^{(n)}(\epsilon) = g^{(n)}(\epsilon)\, d\epsilon \,, \tag{11}$$

where the density $g^{(n)}(\epsilon)$ is the Stieltjes derivative of $f^{(n)}(\epsilon)$,[6]

$$g^{(n)}(\epsilon) = 0, \quad 0 < \epsilon < \epsilon_1(n) \tag{12a}$$

$$g^{(n)}(\epsilon) = \frac{1}{2} \frac{f_{i+1}(n) + f_i(n)}{\epsilon_{i+1}(n) - \epsilon_i(n)} \,, \quad \epsilon_i(n) < \epsilon < \epsilon_{i+1}(n) \tag{12b}$$

$$g^{(n)}(\epsilon) = 0, \quad \epsilon_n(n) < \epsilon \,, \tag{12c}$$

in which case Eq. (6) gives

$$\mathrm{Im}\,\alpha(\omega) = \pi g^{(n)}(\omega)/2\omega + \mathrm{Im}R_n(\omega) \,, \tag{13a}$$

$$\mathrm{Re}\,\alpha(\omega) = \mathrm{P} \int_{\epsilon_1}^{\infty} \frac{g^{(n)}(\epsilon)\, d\epsilon}{\epsilon^2 - \omega^2} + \mathrm{Re}R_n(\omega) \,. \tag{13b}$$

Equation (13a) is directly applicable in the photoionization region $\epsilon_t \leqslant \omega$, whereas in the region of discrete transitions previously described additional considerations are required to extract the appropriate discrete oscillator strengths from $g^{(n)}(\omega)$.[6,8]

C. Tchebycheff procedure

Although the Stieltjes procedure has proved satisfactory in previous applications, it is useful to also investigate convergent approximations to $\alpha(z)$ based on continuous (Tchebycheff) distributions $F^{(n)}(\epsilon)$ and densities $G^{(n)}(\epsilon)$. The Tchebycheff distribution $F^{(n)}(\epsilon)$ is constructed from the solution of the moment problem[9]

$$S(-k) = \epsilon^{-k} f_0(\epsilon) + \sum_{i=1}^{n} \epsilon_i(n, \epsilon)^{-k} f_i(n, \epsilon)$$

$$k = 0, 1, \ldots, 2n \,, \tag{14}$$

where ϵ is an arbitrary preassigned frequency, in the form

$$F^{(n)}(\epsilon) = \sum_i f_i(n, \epsilon) + \tfrac{1}{2} f_0(\epsilon) \,. \tag{15}$$

In Eq. (15) the sum on the right-hand side is over all i for which $0 < \epsilon_i(n, \epsilon) < \epsilon$. We recognize $F^{(n)}(\epsilon)$ as the Stieltjes value of the $(n+1)$-term distribution having a preassigned frequency ϵ, regarded as a function of ϵ.[15] The associated Tchebycheff density is given by

$$G^{(n)}(\epsilon) = \frac{dF^{(n)}(\epsilon)}{d\epsilon} = \sum_i \frac{df_i(n, \epsilon)}{d\epsilon} + \frac{1}{2} \frac{df_0(\epsilon)}{d\epsilon} \,, \tag{16}$$

in which case Eqs. (13) are replaced by

$$\mathrm{Im}\,\alpha(\omega) = \pi G^{(n)}(\omega)/2\omega + \mathrm{Im}R_n(\omega) \,, \tag{17a}$$

$$\mathrm{Re}\,\alpha(\omega) = \mathrm{P} \int_{\epsilon_1}^{\infty} \frac{G^{(n)}(\epsilon)\, d\epsilon}{\epsilon^2 - \omega^2} + \mathrm{Re}R_n(\omega) \,. \tag{17b}$$

It is shown elsewhere that $G^{(n)}(z)$ is continuous and non-negative on the real axis, has $2n-2$ continuous derivatives there, with $2n$ convergent moments

$$S^{(n)}(-k) = \int_{-\infty}^{\infty} \epsilon^{-k} G^{(n)}(\epsilon)\, d\epsilon, \quad k = 0, 1, \ldots, 2n-1 \,, \tag{18}$$

and has conjugate poles in the upper and lower half-planes.[16]

D. Computational aspects

The moment problem of Eq. (8) is linearized through the introduction of Padé approximants[17]

$$[n, n-1](z) = P_{n-1}(z)/Q_n(z) \,, \tag{19a}$$

$$P_{n-1}(z) = \sum_{i=0}^{n-1} a_i^{(n)} z^i \,, \tag{19b}$$

$$Q_n(z) = 1 + \sum_{i=1}^{n} b_i^{(n)} z^i \,, \tag{19c}$$

to the continued fraction[10]

$$A(z) = \cfrac{\beta_0}{1/z - \alpha_1 - \cfrac{\beta_1}{1/z - \alpha_2 - \cdots - \cfrac{\beta_{n-1}}{1/z - \alpha_n - \cdots}}} \tag{20}$$

associated with the Stieltjes integral

$$\beta(z) = \int_{\epsilon_1}^{\infty} \frac{\epsilon\, df(\epsilon)}{\epsilon - z} = S(0) + S(-1)\, z + S(-2)\, z^2 + \cdots \tag{21}$$

up to order $2n-1$:

$$[n, n-1](z) = (1/z) A(z) = \beta(z) = O(z^{2n-1}) \,. \tag{22}$$

Equation (22) provides explicit algorithms for determining the $a_i^{(n)}$, $b_i^{(n)}$ and α_n, β_n from the moments $S(-k)$.[18] When large numbers of moments are employed it is convenient to use the recurrence relations[9]

$$Q_n(z) = (1 - \alpha_n z)\, Q_{n-1}(z) - z^2 \beta_{n-1} Q_{n-2}(z) \,,$$

$$Q_{-1}(z) = 0, \quad Q_0(z) = 1 \,, \tag{23a}$$

$$P_{n-1}(z) = (1-\alpha_n z)\,P_{n-2}(z) - z^2\,\beta_{n-1}\,P_{n-3}(z),$$
$$P_{-1}(z) = 0, \quad P_0(z) = \beta_0\,, \tag{23b}$$

in constructing the polynomials $Q_n(z)$, $P_{n-1}(z)$ orthogonal with respect to the distribution $f(\epsilon)$,[19] and to determine the α_n and β_n appearing in Eqs. (20) and (23) from the moments $S(-k)$ in the forms,[20]

$$\alpha_n = \frac{Y_{n-1,n}}{Y_{n-1,n-1}} - \frac{Y_{n-2,n-1}}{Y_{n-2,n-2}}, \quad \alpha_0 = 0, \quad \alpha_1 = \frac{S(-1)}{S(0)}, \tag{24a}$$

$$\beta_n = \frac{Y_{n,n}}{Y_{n-1,n-1}}, \quad \beta_{-1} = 0, \quad \beta_0 = S(0)\,, \tag{24b}$$

where the matrix elements

$$Y_{n,l} \equiv \int_0^\infty \epsilon^{-l-n}\,Q_n(\epsilon)\,df(\epsilon) \tag{25a}$$

satisfy

$$Y_{n,l} = Y_{n-1,l+1} - \alpha_n\,Y_{n-1,l} - \beta_{n-1}\,Y_{n-2,l}, \tag{25b}$$
$$Y_{n,l} = 0, \quad l < n\,, \tag{25c}$$
$$Y_{0,l} = S(-l)\,, \tag{25d}$$
$$Y_{n,-1} = Y_{-1,l} = 0\,. \tag{25e}$$

The recurrence relation (25b) is obtained directly from Eq. (23a) and the definition of Eq. (25a).

Equations (24) can be written in the alternative forms

$$\alpha_n = \frac{1}{\beta_0\beta_1\cdots\beta_{n-1}} \int_0^\infty \left(\frac{1}{\epsilon}\right)^{2n-1} Q_{n-1}(\epsilon)^2\,df(\epsilon)\,, \tag{26a}$$

$$\beta_n = \frac{1}{\beta_0\beta_1\cdots\beta_{n-1}} \int_0^\infty \left(\frac{1}{\epsilon}\right)^{2n} Q_n(\epsilon)^2\,df(\epsilon)\,, \tag{26b}$$

which are particularly useful when the recurrence coefficients are to be calculated from variationally determined pseudospectra $\tilde{\epsilon}_i$ and $\tilde{f}_i$, $i = 1, N$. In this case, Eqs. (26) become

$$\tilde{\alpha}_n = \frac{1}{\tilde{\beta}_0\tilde{\beta}_1\cdots\tilde{\beta}_{n-1}} \sum_{i=1}^{N} \left(\frac{1}{\tilde{\epsilon}_i}\right)^{2n-1} Q_{n-1}(\tilde{\epsilon}_i)^2\,\tilde{f}_i\,, \tag{27a}$$

$$\tilde{\beta}_n = \frac{1}{\tilde{\beta}_0\tilde{\beta}_1\cdots\tilde{\beta}_{n-1}} \sum_{i=1}^{N} \left(\frac{1}{\tilde{\epsilon}_i}\right)^{2n} Q_n(\tilde{\epsilon}_i)^2\,\tilde{f}_i\,, \tag{27b}$$

where the values $Q_{n-1}(\tilde{\epsilon}_i)$ and $Q_n(\tilde{\epsilon}_i)$ are obtained from the recurrence relations of Eqs. (23) using $\tilde{\alpha}_m$ and $\tilde{\beta}_m$ values of lower order than the $\tilde{\alpha}_n$ and $\tilde{\beta}_n$ being calculated. Equations (23) and (27) provide a convenient stable algorithm for determining $\tilde{\alpha}_n$ and $\tilde{\beta}_n$ values, which is preferable to the use of Eqs. (24) and (25) with spectral moments given by the variationally determined pseudospectra.[21] When the necessary moments are available in closed form, Eqs. (24) and (25) are satisfactory, however.

Once the α_n and β_n are determined from Eqs. (24) and (25) and the known moments [Eq. (5)], or from Eqs. (23) and (27) and variationally determined pseudospectra, Eqs. (23) provide the polynomials $Q_n(z)$ and $P_{n-1}(z)$. The $\epsilon_i(n)$ and $f_i(n)$ are obtained from the roots and residues of $[n, n-1](z)$ [Eqs. (19)–(22)] according to

$$Q_n(\epsilon_i(n)) = 0\,, \tag{28a}$$

$$f_i(n) = \frac{P_{n-1}(\epsilon_i(n))}{\epsilon_i(n)\,Q_n'(\epsilon_i(n))}\,. \tag{28b}$$

The polynomials of Eqs. (23) are also employed to linearize the more general moment problem of Eq. (14). The $\epsilon_i(n, \epsilon)$ and $f_i(n, \epsilon)$ are obtained from roots and residues of the rational fraction

$$\{n, n-1\}(z) = \tilde{P}_{n-1}(z)/\tilde{Q}_n(z)\,, \tag{29a}$$
$$\tilde{P}_n(z) = Q_n(\epsilon)\,P_{n-2}(z) - Q_{n-1}(\epsilon)\,P_{n-1}(z)\,, \tag{29b}$$
$$\tilde{Q}_n(z) = Q_n(\epsilon)\,Q_{n-1}(z) - Q_{n-1}(\epsilon)\,Q_n(z) \tag{29c}$$

according to

$$\tilde{Q}_n(\epsilon_i(n, \epsilon)) = 0\,, \tag{30a}$$

$$f_i(n, \epsilon) = \frac{\tilde{P}_{n-1}(\epsilon_i(n, \epsilon))}{\epsilon_i(n, \epsilon)\,\tilde{Q}_n'(\epsilon_i(n, \epsilon))} \tag{30b}$$

where $\tilde{P}_{n-1}(z)$ and $\tilde{Q}_n(z)$ are the so-called quasi-orthogonal polynomials associated with the distribution $f(\epsilon)$, $\tilde{Q}_n(z)$ having a preassigned root at ϵ.[9]

Equations (19)–(30) show that the polynomials of Eqs. (23) provide the solutions of the moment problems of Secs. II A and II B, emphasizing the importance of the recurrence coefficients α_n and β_n.

III. APPLICATIONS

In this section we apply the Stieltjes and Tchebycheff procedures in determinations of the absorption and dispersion profiles of one- and two-electron atoms and ions.

A. Model ionic system

The continuum oscillator-strength density

$$g(\epsilon) = (8/3\pi)\left[(\epsilon-1)^{1/2}/\epsilon\right]^3, \quad 1 \le \epsilon < \infty\,, \tag{31a}$$

and associated distribution

$$f(\epsilon) = \int_1^\epsilon g(\epsilon')\,d\epsilon'$$
$$= \frac{2}{\pi}\left[\frac{(\epsilon-1)^{1/2}}{3}\left(\frac{2}{\epsilon^2} - \frac{5}{\epsilon}\right) + \tan^{-1}(\epsilon-1)^{1/2}\right] \tag{31b}$$

provides a useful model ionic system for illustrating the Stieltjes and Tchebycheff procedures.[22] The spectral moments [Eq. (5)] in this case are given by

$$S(-k) = \frac{2^{1-2k}(2k)!}{k!(k+2)!}\,, \quad k = 0, 1, \ldots, \tag{32}$$

and the associated recurrence coefficients [Eqs. (24)]

$$\alpha_n = \tfrac{1}{2}(4n^2 - 3)/(4n^2 - 1)\,, \tag{33a}$$

$$\beta_n = \tfrac{1}{4}(2n+3)(2n-1)/(4n+2)^2, \quad \beta_0 = 1\,, \tag{33b}$$

are obtained from solution of Eqs. (25). These can be employed in constructing the polynomials of Eqs. (23) and (29) to arbitrary order, from which the Stieltjes and Tchebycheff approximations [Eqs. (6)–(13) and (14)–(18)] to the photoabsorption and dispersion profiles [Eqs. (1) and (2)] are obtained.[23]

We have evaluated the Stieltjes and Tchebycheff distributions $[f^{(n)}(\epsilon),\ F^{(n)}(\epsilon)]$ and densities $[g^{(n)}(\epsilon),\ G^{(n)}(\epsilon)]$ of Eqs. (7) and (15) and of Eqs. (12) and (16), respectively, for $n = 5, 10, 15, \ldots, 50$, corresponding to the use of 10–100 of the moments of Eqs. (32) in steps of 10. The respective Stieltjes and Tchebycheff distributions and densities are found to be in excellent mutual agreement, and are rapidly convergent to the correct results of Eqs. (31). Distributions and densities obtained employing 100 of the moments of Eqs. (32) are shown in Fig. 1. Although the Tchebycheff bounds on the distribution provided by the Stieltjes histogram are evidently not fully convergent, their mean values, which of course agree with the Tchebycheff distribution, are indistinguishable from the correct result of Eq. (31b). Similarly, the Stieltjes $[g^{(50)}(\epsilon)]$ and Tchebycheff $[G^{(50)}(\epsilon)]$ derivatives are in excellent accord, the latter being indistinguishable from Eq. (31a). Indeed, the moment-theory results obtained employing as few as 20 moments (not shown) are in good agreement with Eqs. (31).[6]

In Fig. 2 are shown the Tchebycheff approximations to the absorption and dispersion profiles of the model ionic system obtained employing 100 of the moments of Eq. (32) and Eqs. (1), (2), and (17). The dispersion profile is evidently in excellent agreement with the correct result

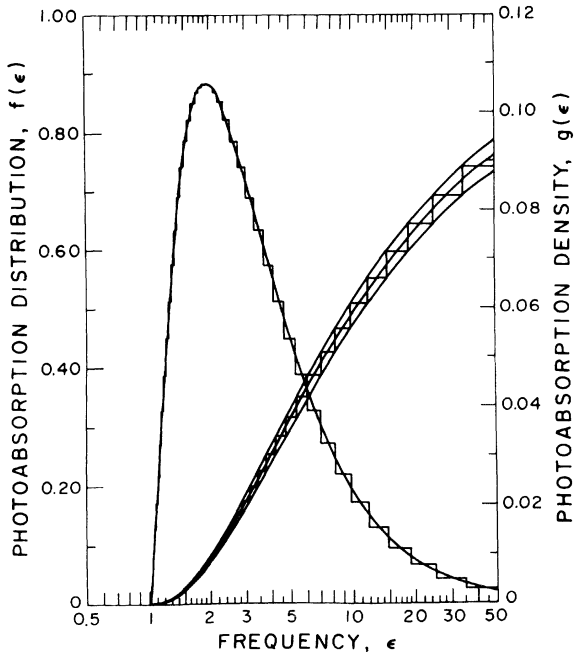

FIG. 1. Stieltjes and Tchebycheff photoabsorption distributions and densities for the negative hydrogen ion in the Bethe-Ohmura approximation obtained employing 100 spectral moments [Eq. (32)] and the development of Sec. II. The Stieltjes results $f^{(50)}(\epsilon), g^{(50)}(\epsilon)$ [Eqs. (7) and (12)] are given by the histograms, and the Tchebycheff results $F^{(50)}(\epsilon), G^{(50)}(\epsilon)$ [Eqs. (15) and (16)] and Tchebycheff bounds (Ref. 15) by the smooth curves. All quantities are dimensionless.

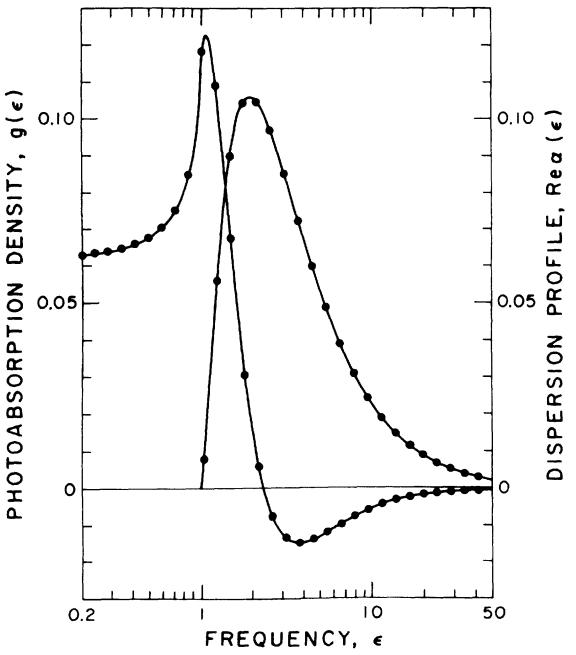

FIG. 2. Photoabsorption and dispersion profiles for the negative hydrogen ion in the Bethe-Ohmura approximation; solid line, Tchebycheff results obtained employing 100 spectral moments [Eq. (32)] and the development of Sec. II; filled circles, correct values obtained from Eqs. (31) and (34). All quantities are dimensionless.

$$\mathrm{Re}\alpha(\omega) = \mathrm{P}\int_1^\infty \frac{g(\epsilon)\,d\epsilon}{\epsilon^2-\omega^2} \tag{34a}$$

$$= (4/3\omega^4)\left[(1+\omega)^{3/2} + (1-\omega)^{3/2} - (\tfrac{3}{4}\omega^2+2)\right],$$

$$0 \le \omega \le 1\,, \tag{34b}$$

$$= (4/3\omega^4)\left[(1+\omega)^{3/2} - (\tfrac{3}{4}\omega^2+2)\right], \quad \omega \ge 1\,, \tag{34c}$$

obtained employing Eq. (31a). As in the case of the absorption profile, the Tchebycheff approximation to the dispersion profile obtained with as few as 20 moments (not shown) is in good accord with the results of Fig. 2,[6] and convergence upon introduction of additional moments is rapid.

The foregoing results demonstrate that the Stieltjes and Tchebycheff procedures can give convergent approximations to continuous photoabsorption and dispersion profiles when the spectral moments necessary for obtaining the recurrence coefficients of Eqs. (23)–(25) are available.

B. Atomic hydrogen

The spectral moments of Eq. (5) for the photoabsorption profile [Eq. (4)] of atomic hydrogen,

$$\epsilon_i = \tfrac{1}{2}[1 - 1/(i+1)^2]\,, \tag{35a}$$

$$f_i = \tfrac{16}{3}(i+1)^{-3}\epsilon_i^{-4}[i/(i+2)]^{2i+2}, \quad i = 1, 2, \ldots, \tag{35b}$$

$$g(\epsilon) = \frac{16}{3}\,\frac{\exp[-4(2\epsilon-1)^{-1/2}\tan^{-1}(2\epsilon-1)^{1/2}]}{\epsilon^4\{1-\exp[-2\pi(2\epsilon-1)^{-1/2}]\}}\,, \quad \epsilon \ge 0.5\,, \tag{35c}$$

can be determined for arbitrary k by a number of methods.[24] The associated recurrence coefficients of Eqs. (23)–(25) in the case of atomic hydrogen are found to take the particularly simple forms[25]

$$\alpha_n = (n+1)/n\,, \tag{36a}$$

$$\beta_n = \tfrac{1}{4}(n+3)/(n+1), \quad \beta_0 = 1\,. \tag{36b}$$

We have used the coefficients of Eqs. (36) in the development of Sec. II to construct the Stieltjes and Tchebycheff distributions $[f^{(n)}(\epsilon),\ F^{(n)}(\epsilon)]$ and densities $[g^{(n)}(\epsilon),\ G^{(n)}(\epsilon)]$ of Eqs. (7) and (15) and of Eqs. (12) and (16), respectively, for $n = 5, 10, 15, \ldots, 40$, corresponding to the use of 10–80 moments in steps of 10.[23] In Figs. 3(a) and 3(b) are shown the Stieltjes and Tchebycheff distribu-

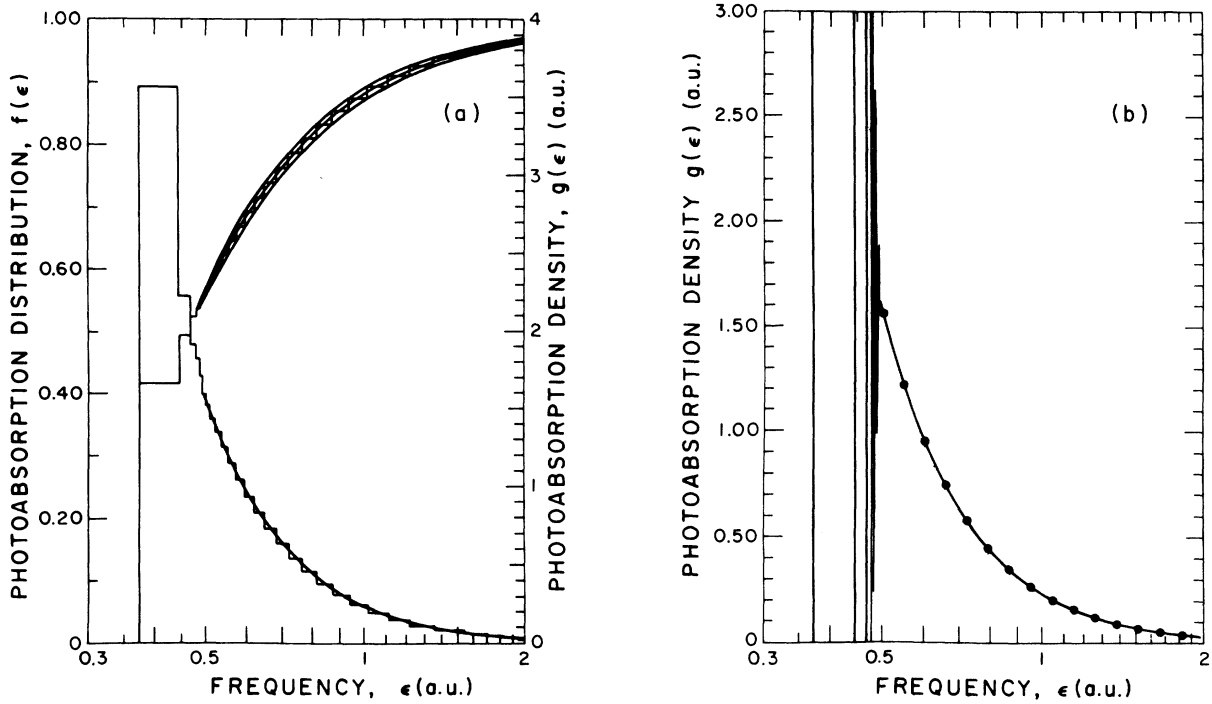

FIG. 3. (a) Stieltjes and Tchebycheff photoabsorption distributions and densities for atomic hydrogen obtained employing 80 spectral moments and the development of Sec. II. The Stieltjes distribution $f^{(40)}(\epsilon)$ [Eq. (7)] is given by the ascending histogram inscribed by the upper and lower Tchebycheff bounds (Ref. 15), and the Stieltjes density $g^{(40)}(\epsilon)$ [Eq. (12)] by the descending histogram. The Tchebycheff distribution $F^{(40)}(\epsilon)$ [Eq. (15)] is given by the indicated mean value of the Tchebycheff bounds, and the Tchebycheff density $G^{(40)}(\epsilon)$ [Eq. (16)] by the smooth curve in the continuum portion of the spectrum. All quantities are in Hartree atomic units. (b) Tchebycheff photoabsorption density $G^{(40)}(\epsilon)$ for atomic hydrogen obtained from the development of Sec. II employing 80 spectral moments. The results in the photoionization continuum are indistinguishable from the correct density of Eq. (35c), indicated by solid circles. All quantities are in Hartree atomic units.

tions and densities obtained employing 80 moments. The results obtained employing fewer spectral moments (not shown) are in good agreement with and rapidly convergent to the results of Figs. 3(a) and 3(b). Evidently, the Tchebycheff bounds on $f(\epsilon)$ shown in Fig. 3(a) are convergent to the correct results in the discrete region, but are not fully convergent in the continuum. However, the mean values of the Stieltjes distribution $[f^{(40)}(\epsilon)]$, which, of course, agree with the Tchebycheff results $[F^{(40)}(\epsilon)]$, are fully convergent to the correct values for all ϵ. The Stieltjes derivative $[g^{(40)}(\epsilon)]$ shown in Fig. 3(a) evidently provides a histogram approximation to the density that is in excellent agreement with the Tchebycheff result $G^{(40)}(\epsilon)$ in the continuum portion of the spectrum. Approximations to the discrete f numbers in atomic hydrogen are obtained directly from the Tchebycheff distribution, and from the Stieltjes density following previously described procedures.[6] In Table I, the first five f numbers in atomic hydrogen obtained from the Stieltjes and Tchebycheff procedures are compared with the exact values, indicating satisfactory mutual agreement. The Tchebycheff derivative $G^{(40)}(\epsilon)$, shown in more detail in Fig. 3(b), evidently exhibits δ-function-like behavior at the correct resonances, and is in excellent agreement with the correct continuum absorption profile above the photoionization threshold. Finally, in Fig. 4 are shown the Tchebycheff

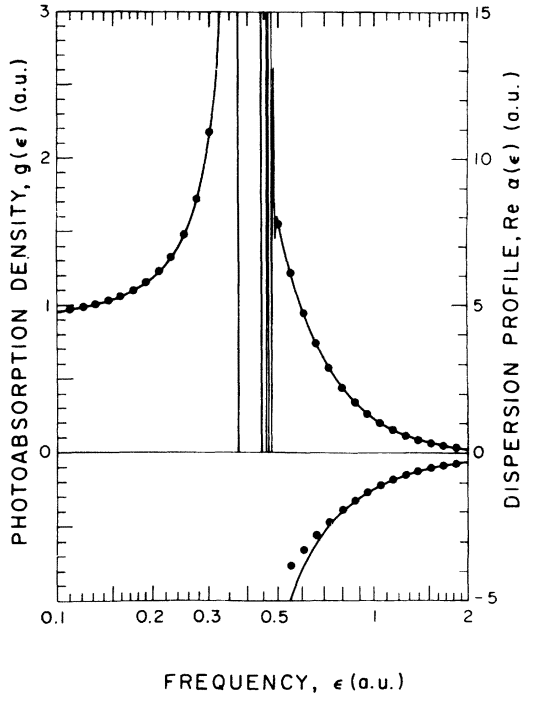

FIG. 4. Photoabsorption and dispersion profiles for atomic hydrogen; solid line, Tchebycheff results obtained employing 80 spectral moments and the development of Sec. II; solid circles, correct values of Eqs. (3) and (35). All quantities are in Hartree atomic units.

TABLE I. Discrete oscillator strengths in atomic hydrogen and helium. [a]

Frequency ϵ_i [b]	Tchebycheff [c]	Stieltjes [d]	Accurate [e]
	Hydrogen		
0.3750	0.4162	0.4161	0.4162
0.4444	0.0791	0.0793	0.0791
0.4688	0.0290	0.0291	0.0290
0.4800	0.0140	0.0140	0.0139
0.4861	0.0080	0.0078	0.0078
	Helium		
0.7797	0.2742	0.2763	0.2761 ± 0.0014 [f]
0.8484	0.0719	0.0733	0.0735 ± 0.0036 [f]
0.8725	0.0207	0.0299	0.0303 ± 0.0071 [f]
0.8836	0.0201	0.0156	0.0148 [g]
0.8897	0.0131	0.0090	0.0084 [g]

[a] Hartree atomic units.

[b] Exact values for atomic hydrogen, experimental values for atomic helium [C. E. Moore, *Atomic Energy Levels*, Natl. Bur. Std. Circ. No. 467 (U. S. GPO, Washington, D. C., 1949), Vol. I].

[c] Values obtained directly from the appropriate Tchebycheff distribution, as discussed in the text.

[d] Values obtained from the appropriate Stieltjes density, following the procedures of P. W. Langhoff, J. Sims, and C. T. Corcoran [Phys. Rev. A 10, 829 (1974)].

[e] Exact values for atomic hydrogen; as indicated for atomic helium.

[f] M. T. Anderson and F. Weinhold, Phys. Rev. A 9, 118 (1974).

[g] L. C. Green, N. C. Johnson, and E. K. Kolchin, Astrophys. J. 144, 369 (1966).

approximations to the photoabsorption and dispersion profiles in atomic hydrogen obtained from the 80-moment results. The dispersion profile has been deleted in the discrete region of the spectrum for clarity. Evidently, the moment-theory profiles shown are in excellent agreement with the correct values, except in the immediate vicinity of the photoionization threshold, where the resolution obtained is limited by the use of finite numbers of moments and evaluation points.[26]

The foregoing results indicate that the Stieltjes and Tchebycheff methods can provide convergent approximations to both discrete and continuum portions of simple photoabsorption and dispersion profiles when the necessary spectral moments are available.

C. Negative hydrogen ion

Approximations to the spectral moments of Eq. (5) in the case of many-electron systems are obtained from variational calculations employing square-integrable basis functions.[6] Ten of the moments obtained from two such independent calculations in the case of the negative hydrogen ion are shown in Table II. Spectrum a uses a 90-term $^1S_0^e$ ground-state function ($E_0 = -0.527\,751\,016$ a.u.) constructed from appropriate configurations of $1s$-$4s$, $1s'$-$3s'$, $2p$, and $3p$ orbitals with optimized Slater exponents multiplied by Hylleraas correlation factors, and a 109-term $^1P_1^o$ pseudospectrum of square-integrable functions constructed from appropriate configurations of $1s$-$6s$, $2p$-$9p$, and $3p'$-$5p'$ orbitals multiplied by Hylleraas factors. Spectrum b corresponds to the use of a 135-term $^1S_0^e$ ground-state function ($E_0 = -0.527\,750\,961$ a.u.) constructed from basis functions of the Perkeris type, and a 110-term $^1P_1^o$ pseudospectrum constructed from correlated functions of the Breit type. In addition, the spectrum-b basis contains the special functions required to satisfy the $S(2)$, $S(1)$, and $S(0)$ sum rules.[11] Although the two calculations are distinct, the first five spectral moments $S(0)$–$S(4)$ in each case shown in Table II agree to within a few parts in the fourth significant figure, and the next five $S(-5)$–$S(-9)$ to within a few parts in the third figure. Moreover, although the pseudospectra of transition frequencies $\tilde{\epsilon}_i$ and oscillator strengths $\tilde{f}_i$ from which the sums of Table II are constructed,[6]

$$\tilde{S}(-k) = \sum_{i=1}^{N} \tilde{\epsilon}_i^{-k} \tilde{f}_i , \tag{37}$$

are different in the two cases, the presence of an inelastic feature corresponding to the $2s$ hydrogenic final state is clearly discernible in both spectra at the appropriate excitation energy (~0.4 a.u.). The appearance of this familiar inelastic feature in the moment-theory spectrum is discussed further below.

TABLE II. Variational approximations to spectral moments for the negative hydrogen ion.[a]

	$S(-k)$	
k	Spectrum a[b]	Spectrum b[b]
0	1.998 057(00)	1.999 998(00)
1	1.494 963(01)	1.496 745(01)
2	2.060 959(02)	2.060 744(02)
3	3.771 499(03)	3.767 879(03)
4	8.010 266(04)	7.994 135(04)
5	1.867 814(06)	1.861 477(06)
6	4.647 274(07)	4.623 764(07)
7	1.213 031(09)	1.204 628(09)
8	3.285 237(10)	3.255 940(10)
9	9.161 894(11)	9.061 453(11)

[a] Values in Hartree atomic units. Numbers in parenthesis refer to appropriate powers of ten.

[b] Values obtained from pseudostate variational calculations employing distinct sets of basis functions (a and b) as discussed in the text.

In Table III the spectrum sum rules $S(2)$, $S(1)$, $S(0)$, $S(-1)$ and Cauchy moments $S(-2)$, $S(-4)$, $S(-6)$, $S(-8)$ obtained from the present calculations are compared with available previous calculations. It is clear that the present results are in good accord with previous accurate calculations, and we can infer that the variationally determined spectral sums provide an accurate representation of the photoabsorption spectrum of the negative hydrogen ion. Note that the spectrum-b sum rules $S(2)$ and $S(1)$ are in excellent agreement with the previous accurate calculations, whereas the corresponding spectrum a results are inaccurate. This is a consequence of including the appropriate special functions in the spectrum-b basis, but not in the spectrum-a basis, as indicated above. Evidently, only the $S(2)$ and $S(1)$ values are significantly affected by the special functions, the other moments from the two pseudospectra being in good accord.

The pseudospectra and first 20 spectral sums in both cases are used to calculate the recurrence coefficients α_n and β_n of Eqs. (23)–(27) shown in Table IV.[27] Evidently, the first five coefficients from the two different spectra are in good mutual agreement, differing by a few parts in the third significant figure, whereas the higher-order spectrum-b coefficients disagree with the spectrum-a results and fail to converge to the correct asymptotic values[28]

$$\alpha_\infty = 1/(2\epsilon_t) , \tag{38a}$$

$$\beta_\infty = 1/(4\epsilon_t)^2 , \tag{38b}$$

where ϵ_t (=0.027 751 a.u.) is the photoionization

TABLE III. Spectral sum rules and Cauchy moments for the negative hydrogen ion. [a]

Spectral sum	Spectrum a [b]	Spectrum b [b]	Previous values
$S(2)$	0.625 74	1.377 59	1.378 54 [c]
$S(1)$	0.713 166	0.747 48	0.747 51 [c]
$S(0)$	1.9981(00)	2.0000(00)	2.0000 [d]
$S(-1)$	1.4950(01)	1.4968(01)	1.496 85(01) [c]
$S(-2)$	2.0610(02)	2.0607(02)	2.0604(02) [e]
$S(-4)$	8.0103(04)	7.9941(04)	8.144(04) [f]
$S(-6)$	4.6473(07)	4.6238(07)	4.672(07) [f]
$S(-8)$	3.2852(10)	3.2560(10)	3.288(10) [f]

[a] All values in Hartree atomic units. Numbers in parenthesis refer to appropriate powers of ten.

[b] See footnote b in Table II.

[c] C. L. Pekeris, Phys. Rev. 126, 1470 (1962).

[d] Thomas-Reiche-Kuhn sum rule.

[e] F. Weinhold, Proc. R. Soc. A327, 209 (1972).

[f] Bethe-Ohmura approximation of Eqs. (32) using the normalization of M. Inokuti and Y.-K. Kim, Phys. Rev. 173, 154 (1968).

threshold frequency. This failure of the spectrum-b recurrence coefficients to converge to the correct limits can be attributed to the generally larger variational pseudostrengths $\bar{f}_i$ obtained (not shown), in this case, relative to the spectrum-a values. Evidently, the basis functions employed in constructing the $^1P_1^o$ psueodspectrum b are less appropriate for spanning the space of the principle pseudostates[6] for the negative hydrogen ion than are the spectrum-a basis functions. As a consequence, the underlying discrete spectrum used to calculate the sums of Table II makes its presence felt in the α_n and β_n values for $n \geq 9$ in the case of the spectrum b, whereas the spectrum-a results, obtained with a distrubution of smaller $\bar{f}_i$ values, are found to be reliable for $n \leq 13$. Of course, the α_n and β_n coefficients obtained from any finite variational calculation will fail to converge to the values of Eqs. (38) for sufficiently large n.

TABLE IV. Polynomial recurrence coefficients for the dipole spectrum of the negative hydrogen ion. [a]

	Spectrum a		Spectrum b	
n	α_n	β_{n-1}	α_n	β_{n-1}
1	7.482 08	1.998 06	7.483 73	2.000 00
2	16.174 92	47.166 56	16.178 02	47.031 06
3	17.540 44	64.744 53	17.515 33	64.262 50
4	17.814 89	71.047 96	17.859 73	70.475 42
5	17.782 46	75.468 19	17.954 06	74.513 59
6	17.736 32	78.449 70	17.950 09	76.274 44
7	17.816 85	79.783 05	17.942 83	77.953 84
8	18.042 87	79.253 22	17.200 83	80.632 89
9	18.184 08	77.925 61	9.886 99	72.496 30
10	18.248 69	77.561 84	1.236 42	1.511 00
∞ [b]	18.017 68	81.159 16	18.017 68	81.159 16

[a] Values in Hartree atomic units obtained from Eqs. (23) to (27) and variationally determined pseudospectra.

[b] Asymptotic limits obtained from Eqs. (38) as discussed in the text, where $\epsilon_t = 0.027\,751$ a.u. is the threshold frequency for photoionization in this case.

The recurrence coefficients of Table IV are employed in constructing the Stieltjes and Tchebycheff distributions and densities corresponding to the use of up to 20 moments for each spectrum. The Stieltjes results obtained for both spectra are in excellent mutual agreement for a given number of moments, and are convergent to smooth profiles as the number of moments employed is increased, whereas the Tchebycheff results, although in excellent mutual accord and in agreement with the Stieltjes values using up to 16 moments, fail to converge in the case of the spectrum-b results when additional moments beyond 16 are employed. This failure to converge is a consequence of employing the coefficients α_9, β_9, and α_{10}, β_{10} in the spectrum-b calculations. When these are introduced, although the Stieltjes density $g^{(20)}(\epsilon)$ is convergent, the Tchebycheff density $G^{(20)}(\epsilon)$ exhibits large peaks and deep minima, reflecting the underlying discrete spectrum employed in the calculation of the spectral sums. By contrast, it is found that approximately 30 of the spectrum-a sums can be employed in the Tchebycheff approach (not shown) before the presence of the underlying discrete pseudospectrum is evident.

Although the Stieltjes and Tchebycheff results obtained from the coefficients of Table IV are satisfactory, it is useful to supplement these with additional values for higher n that are compatible with the known asymptotic limits α_∞ and β_∞ [Eqs.

(38)], in order to extend the moment methods to higher order. The coefficients of Table IV are well approximated by the simple expressions[29]

$$\alpha_n = \alpha_\infty(1+\delta_1/n+\delta_2/n^2), \tag{39a}$$

$$\beta_n = \beta_\infty[1+\gamma_1/(n+1)+\gamma_2/(n+1)^2], \tag{39b}$$

with (spectrum a, spectrum b)

$$\delta_1 = 0.175\,64,\ 0.176\,23,\quad \delta_2 = -0.760\,37,\ -0.760\,88, \tag{40a}$$

$$\gamma_1 = -0.144\,92,\ -0.191\,69,\quad \gamma_2 = -1.385\,52,\ -1.298\,65, \tag{40b}$$

obtained by fitting Eqs. (39) to the first two coefficients α_1, α_2 and β_1, β_2 in each case. Since the latter values obtained from the two spectra are in good mutual agreement (Table I), Eqs. (39) and (40) provide a unique set of recurrence coefficients with which to extend the values of Table IV.

The coefficients of Table IV and Eqs. (39) and (40) are employed in the Tchebycheff procedure of Sec. II in constructing the fully convergent photoabsorption profile for the negative hydrogen shown in Fig. 5. Evidently, the results so obtained are in excellent agreement with the available measurements, normalized to our results at 0.086 29 a.u., and with previous continuum wave-function calculations for frequency below the 2s inelastic threshold.[4] In the latter region, the Tchebycheff results indicate the presence of the inelastic contribution to the total photoabsorption profile.[30] It is important to recognize that the results of Fig. 5, obtained using the ten spectrum-a coefficients of Table IV and ten of the coefficients of Eqs. (39) for $10 < n \leq 20$, are in good accord with the Tchebycheff results obtained from the first 20 coefficients of Eqs. (39) and (40). Thus the purpose of the coefficient extension of Eqs. (39) is to enforce the correct asymptotic behavior of α_n and β_n, which essentially places the threshold of the density at the appropriate value. The shape of the density is determined from the lower-order coefficients or spectral moments. Indeed, the coefficients of Eqs. (39) are obtained from the first five spectral moments of Table II and the photoionization threshold frequency.[31]

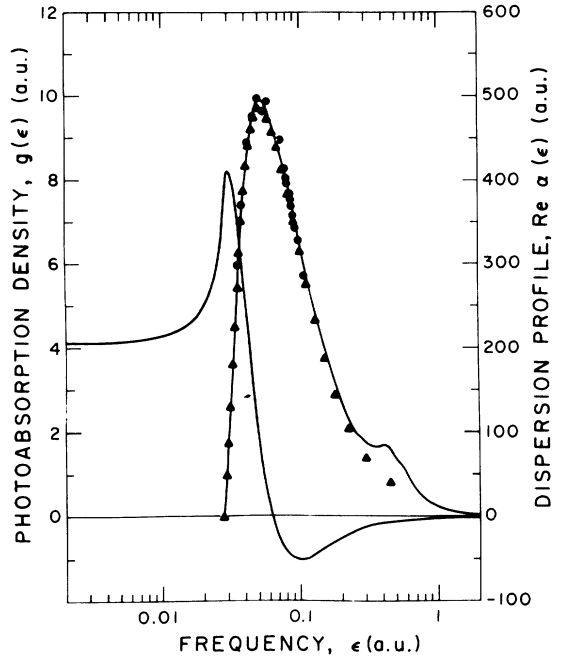

FIG. 5. Photoabsorption and dispersion profiles in the negative hydrogen ion; solid line, Tchebycheff results obtained from the coefficients of Table IV and the development of Sec. II, as discussed in the text; solid circles, experimental data [S. J. Smith and D. S. Burch, Phys. Rev. 116, 1125 (1959)] normalized to the Tchebycheff results at $\epsilon = 0.086\,29$ a.u.; solid triangles, accurate theoretical calculations obtained employing continuum wave functions [S. Geltman, Astrophys. J. 136, 935 (1962); N. A. Doughty, P. A. Fraser, and R. P. McEachran, Mon. Not. R. Astron. Soc. 132, 255 (1966)]. All quantities are in Hartree atomic units.

D. Atomic helium

Basis functions similar in type to those employed above for the negative hydrogen ion are employed in constructing appropriate $^1S_0^e$ ground-state wave functions and $^1P_1^o$ pseudostates for atomic helium. The spectrum a, spectrum b ground-state energies obtained are $-2.903\,723\,99$, $-2.903\,724\,37$, and associated spectral moments obtained from both the correlated configuration basis and the Pekeris basis are compared in Table V. Evidently, the two sets of values are in excellent mutual accord, suggesting that the special basis functions employed in the spectrum-b calculation affect only the $S(2)$, $S(1)$, and $S(0)$ values, and not the negative-integer moments. In contrast to the corresponding values for the negative hydrogen ion, the higher moments of Table V are in better mutual agreement than are the lower ones. Indeed, the two $S(-9)$ values differ by only one part in the fourth significant figure. This does not necessarily imply that the values of Table V are *a priori* more accurate than those of Table II. Rather, in the case of atomic helium the first discrete oscillator strength dominates the higher-order $S(-k)$ values, and contributions from the rest of the spectrum are contained in higher significant figures.

In Table VI the spectral sum rules and Cauchy moments obtained from the present calculations are compared with previous accurate calculations and semiempirical and experimental values. There is evidently excellent mutual agreement, except

TABLE V. Variational approximation to spectral moments for atomic helium. [a]

k	$S(-k)$ Spectrum a [b]	Spectrum b [b]
0	1.992 526	2.000 000
1	1.504 771	1.504 994
2	1.383 019	1.381 584
3	1.414 911	1.413 573
4	1.542 067	1.541 327
5	1.749 849	1.749 589
6	2.040 661	2.040 570
7	2.426 460	2.426 220
8	2.926 768	2.926 124
9	3.568 743	3.567 512

[a] Values in Hartree atomic units.
[b] See footnote b of Table II.

in the case of the $S(2)$ and $S(1)$ values, a consequence of the lack of special functions in the spectrum-a calculation. Nevertheless, the spectrum-a negative-integer sums are in excellent agreement with the other values.

The moments of Table V and the related pseudospectra are used in Eqs. (23)–(27) to calculate the recurrence coefficient for atomic helium shown in Table VII.[27] Evidently, the first five coefficients obtained from the two spectra are in good mutual agreement, whereas the higher-order coefficients oscillate about the correct asymptotic values, and are in poor mutual agreement. As in the case of the negative hydrogen ion, the coefficients of Table VII that are in good agreement are well represented by Eqs. (39), where, in this case (spectrum-a, spectrum-b),

$$\delta_1 = 1.036\,81,\ 1.054\,68,\quad \delta_2 = -0.671\,36,\ -0.694\,13, \tag{41a}$$

$$\gamma_1 = 0.759\,65,\ 0.564\,26,\quad \gamma_2 = 0.954\,16,\ 1.385\,51. \tag{41b}$$

The δ_i and γ_i of Eqs. (41) are obtained from the first two α_n and β_n of Table VII, and are determined uniquely, therefore, by the first five spectral moments of Table V and the known threshold

TABLE VII. Polynomial recurrence coefficients for the dipole spectrum of atomic helium. [a]

n	Spectrum a α_n	Spectrum a β_{n-1}	Spectrum b α_n	Spectrum b β_{n-1}
1	0.755 208	1.992 526	0.752 497	2.000 000
2	0.746 974	0.123 765	0.748 768	0.124 540
3	0.699 890	0.103 948	0.692 243	0.102 632
4	0.695 875	0.093 637	0.667 668	0.103 021
5	0.707 686	0.077 095	0.603 775	0.082 381
6	0.562 169	0.082 382	0.522 282	0.159 888
7	0.586 662	0.128 016	0.846 869	0.041 963
8	0.759 833	0.058 341	0.375 453	0.103 925
9	0.495 706	0.071 810	0.866 257	0.037 371
10	0.689 247	0.104 143	0.408 967	0.116 208
∞ [b]	0.553 082	0.076 475	0.553 082	0.076 475

[a] Values in Hartree atomic units obtained from Eqs. (23) to (27) and variationally determined pseudospectra.
[b] Asymptotic limits obtained from Eqs. (38), where $\epsilon_t = 0.904\,025$ a.u. is the threshold frequency for photoionization in this case.

TABLE VI. Spectral sum rules and Cauchy moments for atomic helium. [a]

Spectral sum	Spectrum a [b]	Spectrum b [b]	Previous values
$S(2)$	12.1120	30.3342	30.3325 [c]
$S(1)$	3.7690	4.0837	4.0837 [c]
$S(0)$	1.9925	2.0000	2.0000 [d]
$S(-1)$	1.5048	1.5050	1.505 [c]
$S(-2)$	1.3830	1.3816	1.3832 [e]
$S(-4)$	1.5421	1.5413	1.5461 ± 0.0001 [f]
$S(-6)$	2.0407	2.0406	2.042 ± 0.006 [f]
$S(-8)$	2.9268	2.9261	2.95 [g]

[a] Values in Hartree atomic units.
[b] See footnote b of Table II.
[c] C. L. Pekeris, Phys. Rev. 112, 1649 (1958).
[d] Thomas-Reiche-Kuhn sum rule.
[e] A. D. Buckingham and P. G. Hibbard, Symp. Faraday Soc. 2, 41 (1968).
[f] G. Starkschall and R. G. Gordon, J. Chem. Phys. 54, 663 (1971). Our calculated $S(-2)$ and $S(-4)$ values are incompatible with the bounds of these authors [the reported $S(-2)$ bounds are 1.3849 ± 0.0001]. The bounds are not rigorous, however, and should be weakened by including larger uncertainties in the theoretical and experimental absorption and dispersion data used in the author's development. Specifically, the errors in the calculations of C. Schwartz [Phys. Rev. 123, 1700 (1961)] are significantly underestimated by Starkschall and Gordon.
[g] P. W. Langhoff and M. Karplus, J. Opt. Soc. Am. 59, 863 (1969).

frequency for photoionization. Note that the coefficients of Table VII converge to their asymptotic values from above, whereas those of Table IV converge to their asymptotic values from below.[32]

The recurrence coefficients of Table VII and Eqs. (39) and (41) are employed in constructing Stieltjes and Tchebycheff photoabsorption and dispersion profiles for atomic helium. As in the case of the negative hydrogen ion, when the higher-order recurrence coefficients of Table VII are employed, the resulting Tchebycheff spectra exhibit large peaks and deep minima, indicating the presence of the underlying discrete variational spectrum, although the Stieltjes spectra, corresponding to a greater degree of smoothing, are somewhat more stable in higher order. This difficulty is avoided by using the coefficients of Eqs. (39) and (41), which correctly incorporate the accurately computed low-order spectral moments of Table V and the correct asymptotic limits of Eqs. (38). In Fig. 6 are shown the convergent Tchebycheff results, employing 20 of the coefficients of Eqs. (39) and (41), in comparison with experimental measurements of photoabsorption and dispersion in atomic helium. As in atomic hydrogen,

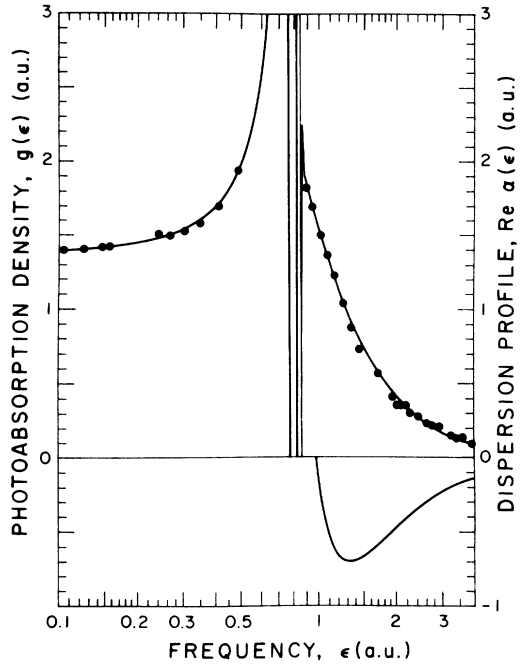

FIG. 6. Photoabsorption and dispersion profiles in atomic helium; solid line, Tchebycheff results obtained from 20 of the coefficients of Eqs. (39) and (41) and the development of Sec. II; solid circle, experimental absorption data of J. A. R. Sampson, Adv. At. Mol. Phys. 2, 177 (1966), and dispersion data of C. Cuthbertson and M. Cuthbertson, Proc. R. Soc. Lond. 135, 90 (1932), and M. C. E. Huber and G. Tondello, J. Opt. Soc. Am. 64, 390 (1974). All quantities are in Hartree atomic units.

the dispersion profile is deleted in the discrete spectrum for clarity. Evidently, the agreement between the moment-theory results and the measured absorption and dispersion data is excellent. Moreover, the results of Fig. 6 are in good agreement with the previously described Stieltjes result,[6] and with accurate calculations employing continuum wave functions.[4] The discrete f numbers in atomic helium are obtained directly from the Tchebycheff distribution, and from the previously described Stieltjes approach.[6] The first five discrete oscillator strengths so obtained are compared with previous theoretical calculations[4] in Table I. Here, the Tchebycheff results are less satisfactory than in the case of atomic hydrogen, where a larger number of accurate moments is employed, although the Stieltjes results are in good agreement with available accurate calculations. The Tchebycheff results in Table I can be improved significantly by the use of additional moments or recurrence coefficients. In this case, however, as indicated above, the continuum portion of the moment-theory spectrum can be unstable unless the moment extension of Eqs. (39) is employed. The previously described reference-density approach can be employed as a complementary alternative to the Stieltjes and Tchebycheff procedures for determining discrete oscillator strengths.[33]

IV. CONCLUDING REMARKS

The Stieltjes and Tchebycheff moment methods have provided accurate approximations to photoabsorption and dispersion profiles in simple one- and two-electron atoms and ions. Variational calculations of a conventional type provide the necessary spectral moments in the case of two-electron systems, whereas the moments for one-electron systems are obtained in closed forms. The moment problems that arise in constructing the Stieltjes and Tchebycheff distributions and densities are solved by evaluating the polynomials orthogonal and quasiorthogonal with respect to the correct densities. Well-known algorithms of Stieltjes and Tchebycheff, and a simple moment-extension technique employing known asymptotic values, allow the construction of the associated polynomial recurrence coefficients and their extension to infinite order. The resulting absorption and dispersion profiles obtained for the systems studied are in excellent agreement with the appropriate exact results, experimental measurements, and previous calculations employing discrete and continuum wave functions. These results suggest that the Stieltjes and Tchebycheff moment methods should provide useful approximations to photoabosrption and dispersion profiles in atoms and molecules of arbitrary complexity.[34]

ACKNOWLEDGMENTS

Acknowledgment is made of the Camille and Henry Dreyfus Foundation, the Proctor and Gamble Corporation, the JILA Visiting Fellow Program, the National Science Foundation, and of the donors of The Petroleum Research Fund, administered by the American Chemical Society, for partial support of this work. It is a pleasure to thank various colleagues, particularly V. McKoy, W. P. Reinhardt, E. J. Heller, and R. K. Nesbet, for communicating their results prior to publication.

---

[1]Theoretical aspects of absorption and dispersion profiles are reviewed, for example, by U. Fano and J. W. Cooper, Rev. Mod. Phys. 40, 441 (1968), and P. W. Langhoff, S. T. Epstein, and M. Karplus, *ibid.* 44, 602 (1972), respectively. Experimental absorption and dispersion data, respectively, are tabulated, for example, by J. A. R. Samson, Adv. At. Mol. Phys. 2, 177 (1966), and H. H. Landolt and B. Börnstein, *Zahlenwerte und Funcktionen* (Springer, Berlin, 1962), Vol. 2, Chap. 8.

[2]A critical review of photoabsorption measurements and calculations is given by L. M. Branscomb, *Physics of One- and Two-Electron Atoms* (North-Holland, Amsterdam, 1969).

[3]H. A. Bethe and E. E. Salpeter, *Quantum Mechanics of One- and Two-Electron Atoms* (Springer, Berlin, 1957).

[4]Accurate conventional calculations for two-electron systems that avoid the approximations required for larger atoms and molecules are reported, for example, by B. Schiff and C. L. Pekeris, Phys. Rev. 134, A638 (1964); L. C. Green, N. C. Johnson, and E. K. Kolchin, Astrophys. J. 144, 369 (1966); M. T. Anderson and F. Weinhold, Phys. Rev. A 9, 118 (1974), for discrete absorption in atomic helium; by P. G. Burke and D. D. McVicar, Proc. Phys. Soc. Lond. 86, 989 (1965); K. L. Bell and A. E. Kingston, *ibid.* 90, 31 (1967); V. Jacobs, Phys. Rev. A 3, 289 (1971), for photoionization in atomic helium; by K. T. Chung, Phys. Rev. 166, 1 (1968), for normal dispersion in atomic helium; by S. Geltman, Astrophys. J. 136, 935 (1962); N. A. Doughty, P. A. Fraser, and R. P. McEachran, Mon. Not. Roy. Astron. Soc. 132, 255 (1966), for photoionization in the negative hydrogen ion; and by K. T. Chung, Phys. Rev. A 4, 7 (1971), for normal dispersion in the negative hydrogen ion.

[5]P. W. Langhoff, Chem. Phys. Lett. 9, 89 (1971); J. Chem. Phys. 57, 2604 (1972).

[6]P. W. Langhoff, Chem. Phys. Lett. 22, 60 (1973); P. W. Langhoff and C. T. Corcoran, J. Chem. Phys. 61, 146 (1974); P. W. Langhoff, J. Sims, and C. T. Corcoran, Phys. Rev. A 10, 829 (1974).

[7]Nonconventional techniques for photoabsorption calculations that employ only square-integrable basis functions have been devised independently by a number of workers. J. T. Broad and W. P. Reinhardt [J. Chem. Phys. 60, 2182 (1974)] have reported the use of analytic continuation of complex dynamic polarization calculations. T. N. Rescigno, C. W. McCurdy, Jr., and V. McKoy [Phys. Rev. A 9, 2409 (1974); J. Chem. Phys. 64, 477 (1976)] have applied the so-called coordinate-rotation method in this connection, H. A. Yamani and W. P. Reinhardt [Phys. Rev. A 11, 1144 (1975)] have suggested an "equivalent-quadrature" approach to photoionization calculations, and E. J. Heller [Phys. Rev. A 12, 1222 (1975)] has described a J-matrix approach to photoabsorption calculations. Comments are made at appropriate points below on connections between these approaches and the moment-theory methods employed in the present development.

[8]A general review of the Stieltjes moment approach for imaging spectral densities in various contexts is given by P. W. Langhoff, Int. J. Quantum Chem. S8, 347 (1974).

[9]J. A. Shohat and J. D. Tamarkin, *The Problem of Moments* (American Mathematical Society, Providence, 1943).

[10]H. S. Wall, *Analytic Theory of Continued Fractions* (Van Nostrand, New York, 1948).

[11]A. Dalgarno and S. T. Epstein, J. Chem. Phys. 50, 2877 (1969).

[12]G. V. Marr, *Photoionization Processes in Gases* (Academic, New York, 1967), pp. 7 and 33.

[13]S. A. Korff and G. Breit, Rev. Mod. Phys. 4, 471 (1932).

[14]J. O. Hirschfelder, W. Byers-Brown, and S. T. Epstein, Adv. Quantum Chem. 1, 256 (1964).

[15]The Stieltjes values of a distribution of the form of Eqs. (7), constructed according to Eq. (8), are the mean vlaues of the left- and right-hand limits at the points of increase $\epsilon_i(n)$. The distribution of Eq. (14), with a preassigned frequency at arbitrary ϵ, thus provides Stieltjes values over the entire frequency range [Eq. (15)], and, moreover, provides upper and lower Tchebycheff bounds on $f(\epsilon)$ for all ϵ. For an alternative application of the Tchebycheff distribution, see, K. B. Winterbon, J. Chem. Phys. 53, 1302 (1970); Atomic Energy of Canada, Ltd. Report No. 4832, 1974 (unpublished).

[16]C. T. Corcoran, Ph.D. thesis (Indiana Univ., 1976) (unpublished). The moments of Eq. (18) are in good agreement with but do not exactly reproduce the input moments of Eq. (5), except in the limit of large n, in which case convergence is obtained. The fact that $G^{(n)}(z)$ has poles in the upper and lower half-planes suggests a connection with the coordinate-rotation method in a finite basis (Ref. 7). Numerical studies in the case of atomic hydrogen and the negative ion in the Bethe-Ohmura approximation [P. W. Langhoff and C. T. Corcoran, Chem. Phys. Lett. (to be published)] indicate that the poles obtained lie along a ray similar to the rotated photoionization cut obtained from the coordinate-rotation method. Moreover, in the case of atomic helium, a second cut associated with the first inelastic channel $1s^2 \rightarrow 2skp$ is also discernible.

[17]G. A. Baker, Jr., *Essentials of Padé Approximants* (Academic, New York, 1975).

[18]Any of a number of closely related procedures can be employed in determining the $a_i^{(n)}, b_i^{(n)}$ and α_n, β_n when small ($\lesssim 30$) numbers of moments are available. See, for example, R. G. Gordon, J. Math. Phys. 9, 655 (1968); P. W. Langhoff and M. Karplus, Phys. Rev. Lett. 19, 1461 (1967); J. Chem. Phys. 52, 1435 (1970). It is perhaps useful to note that the $a_i^{(n)}$ and $b_i^{(n)}$ are dependent upon the order of truncation of the continued fraction, necessitating the superscript n, whereas the α_n and β_n are not dependent upon the order of truncation. Moreover, the continued fraction of Eq. (20) can be written in a number of equivalent forms involving sequences of coefficients related to the α_n and β_n, as is discussed in detail in Ref. 10. The latter are convenient to employ, since they appear directly in the recurrence relation for the polynomials orthogonal with respect to $f(\epsilon)$.

[19]Upon introduction of the variable $x = 1/\epsilon$ and the polynomials $q_n(x) \equiv x^n Q_n(1/x)$, Eq. (23a) takes the form $q_n(x) = (x - \alpha_n) q_{n-1}(x) - \beta_{n-1} q_{n-2}(x)$. The $q_n(x)$ are the customary (Ref. 9) monic polynomials orthogonal with respect to the density $F(x) = S(0) - f(\epsilon)$, which has the spectral moments $S(-k)$ [Eq. (5)] as positive-integer power moments. Similarly, $p_n(x) \equiv x^{(n-1)} P_{n-1}(1/x)$ is the customary numerator polynomial of degree $n-1$ and order n associated with the denominator polynomial $q_n(x)$, and satisfies the same recurrence relation as the latter. We refer in the present development to the $Q_n(\epsilon)$ and $P_{n-1}(\epsilon)$ as the polynomials orthogonal with respect to $f(\epsilon)$, although it is perhaps important to recognize that this is the case when the appropriate variable $1/\epsilon$ is introduced.

[20]The algorithm of Eqs. (24) and (25) is a variant of those devised originally by Stieltjes and Tchebycheff, cited and described in Chap. XI of Ref. 10. The Stieltjes form has been employed previously by J. Deltour [Physica (Utr.) 39, 413 (1968)] in Stieltjes imaging distributions of normal-mode vibrations in crystals, and C. Blumstein and J. C. Wheeler [Phys. Rev. B 8, 1764 (1973)] have employed a form of Eqs. (24) and (25) in conjunction with the use of modified (polynomial) moments in imaging spectral densities for crystal lattice vibrations. The latter authors, who cite a number of additional pertinent references, do not employ the Stieltjes or Tchebycheff derivatives of the present development, but, rather, express the unknown spectral density as the product of a known reference density and an expansion in the associated orthogonal polynomials. The development is a logical extension and improvement of the expansion in Legendre polynomials originally employed by E. W. Montroll [J. Chem. Phys. 10, 218 (1942); 11, 481 (1943)] in the normal-mode problem. It is perhaps of interest to note that when the approximate density of Blumstein and Wheeler is evaluated at the roots of the polynomials orthogonal with respect to the known reference density employed, results identical with the equivalent-quadrature method of H. A. Yamani and W. P. Reinhardt, cited in Ref. 7, are obtained. Moreover, Blumstein and Wheeler correctly note that the use of modified moments results in a more stable moment problem than that encountered using power moments, but that in the latter case the algorithm of Eqs. (24) and (25) is superior to the so-called product-difference and quotient-difference algorithms. In the present development, the instability of Eqs. (24) and (25) when large numbers of moments are employed is avoided by noting that the α_n and β_n rapidly approach their asymptotic values α_∞ and β_∞, which are determined by the known frequency threshold for photoionization, as is discussed further below. In a separate development, R. G. Gordon [Adv. Chem. Phys. 15, 79 (1968)] has noted that the continued fraction of Eq. (20) can be summed to infinite order when the α_n and β_n are replaced by their asymptotic values α_∞ and β_∞ beyond a given order. This approach provides an approximate dispersion integral [Eq. (21)] having a finite number of poles and a square-root branch cut, which is appropriate in the normal-mode problem, but generally inappropriate for the photoabsorption problem considered here.

[21]Recently, R. K. Nesbet (private communication) and W. P. Reinhardt and co-workers (private communication) have explored the possibility of direct quantum-mechanical calculations of α_n and β_n values appropriate for photoabsorption densities which do not involve the diagonalizations necessary for constructing pseudospectra $\tilde{\epsilon}_i$, $\tilde{f}_i$, and without apparent recourse to spectral moments or the algorithm of Eqs. (24) and (25). The Nesbet development is evidently a generalization of Eqs. (27) to the case of a nondiagonal transition energy matrix.

[22]See, for example, M. Inokuti and Y.-K. Kim, Phys. Rev. 173, 154 (1968), and references cited therein. The density of Eq. (31a) is of the Jacobi type in an appropriate variable, and, consequently, the polynomials of Eqs. (23) in this case are related to well-known classical orthogonal polynomials. See, for example, U. W. Hochstrasser, in *Handbook of Mathematical Functions*, edited by M. Abramowitz and I. A. Stegun, (U.S. GPO, Washington, D.C., 1964), Chap. 22. More generally, the polynomials of Eqs. (23) are not related to classical polynomials, but rather are simply those orthogonal with respect to the associated photoabsorption density. It is perhaps of interest to note in this connection that the Jacobi-matrix approach of E. J. Heller and the equivalent-quadrature method of H. A. Yamani and W. P. Reinhardt, cited in Ref. 7, are restricted to those cases in which the appropriate recurrence equations in each case can be solved in analytic forms. Although the Jacobi-matrix designation of Heller is apparently independently motivated, it is in accord with the more traditional use of the term, as employed, for example, by H. S. Wall, Ref. 10, p. 226.

[23]Although we have not discussed it in detail in Sec. II C, the Tchebycheff derivative can be evaluated at any of the steps of an n-term histogram having a prespecified frequency point. When 40 spectral moments are employed, for example, a 20-step histogram is obtained which provides the Tchebycheff derivative at 20 distinct frequency values. The construction of 50 such histograms therefore provides 1000 data points for the photoabsorption profile, the entire calculation requiring approximately 10 sec CPU time on the CDC 6600 computer. Evaluation of the dispersion integral of Eq. (17b) is aided by analytic treatment of the principal-value contribution using methods similar to the dispersion-correction technique of E. J. Heller, T. N.

Rescigno, and W. P. Reinhardt [Phys. Rev. A 8, 2946 (1973)].

[24]See, for example, R. J. Bell, Proc. Phys. Soc. Lond. 92, 842 (1967). In a separate development [P. W. Langhoff and D. J. Margoliash (unpublished)] we have evaluated the spectral sums appropriate for the generalized oscillator-strength distribution in atomic hydrogen employing a number of procedures, and have constructed Stieltjes and Tchebycheff densities for the associated Bethe surface. The dipole sums and oscillator-strength distribution are obtained from the generalized values in the limit of zero momentum transfer.

[25]The polynomials of Eqs. (23) in the case of atomic hydrogen are apparently related to the attractive Coulomb-Pollaczek polynomials discussed by H. A. Yamani and W. P. Reinhardt in Ref. 7. For a description of the classical Pollaczek polynomials see, for example, G. Szego, *Orthogonal Polynomials* (American Mathematical Society, Providence, 1959).

[26]In Figs. 3(b) and 4 the resolution of the photoabsorption densities shown is limited at the photoionization threshold by the number of points at which the necessary polynomials [Eqs. (23) and (29)] and related quantities are evaluated, whereas the accuracy of the associated dispersion profile is determined by the number of moments employed and the nature of the dispersion correction technique employed. Moreover, unless a fine mesh of points is employed in evaluating the Tchebycheff density, it is possible to miss the very narrow δ-function-like peaks associated with the lowest resonances. Of course, the discrete transitions are easily discernible, in general, in the associated Tchebycheff distribution.

[27]The recurrence coefficients of Tables IV and VII are calculated from the algorithms both of Eqs. (24) and (25) and of Eqs. (23) and (27), the values of Eq. (37) being employed in the former case. Good mutual agreement is obtained from the two procedures for the coefficients shown in the tables, although the development based on Eqs. (23) and (27) is preferable for the calculation of higher-order recurrence coefficients.

[28]H. S. Wall, Ref. 10, p. 209.

[29]Equations (39) are suggested by the asymptotic forms of the known recurrence coefficients for the previously studied model ionic system [Eqs. (33)] and atomic hydrogen [Eqs. (36)]. We have found that the resulting densities and distributions obtained from extended coefficients are relatively insensitive to the specific functional form employed, provided that the correct asymptotic values are obtained in the limit $n \to \infty$, and that convergence to these values is rapid. Moreover, in certain instances the extrapolation of variationally calculated recurrence coefficients to the known asymptotic values is more conveniently accomplished using an alternative representation of the continued fraction of Eq. (20).

[30]J. Macek, Proc. Phys. Soc. Lond. 92, 365 (1967). Recently, J. T. Broad and W. P. Reinhardt [Chem. Phys. Lett. 37, 212 (1976), and unpublished] have made a detailed study of the photoabsorption profile in the hydrogen ion, including the line shapes near the 2*s* threshold, employing the J-matrix approach and various procedures described in the references of footnotes 6 and 7. Alternative bound-state procedures for calculating resonance and nonresonance contributions to photoabsorption profiles are described by R. F. Stewart, C. Laughlin, and G. A. Victor [Chem. Phys. Lett. 29, 353 (1974)], H. Doyle, M. Oppenheimer, and A. Dalgarno [Phys. Rev. A 11, 909 (1975)], and M. Oppenheimer and H. Doyle [Phys. Rev. A 13, 665 (1976)].

[31]This suggests that very small numbers of spectral moments, obtained from theoretical calculations, semiempirical procedures, experimental data, and known photoionization thresholds, can be employed in obtaining Tchebycheff approximations to photoabsorption profiles in atoms and molecules of arbitrary complexity. The use of semiempirical and experimental spectral moments in the Tchebycheff procedure is pursued separately.

[32]Although a detailed discussion is beyond the scope of the present development, it is important to recognize that the behavior of the α_n and β_n, and related sequences of coefficients, are largely determined by the threshold frequency for photoionization and the qualitative form of the photoabsorption profile under investigation. A number of model studies indicate that complex spectra give rise to oscillatory behavior in the α_n and β_n of such forms that separation into subsequences is possible, in which connection investigation of the related minimal chain sequences discussed by H. S. Wall, Ref. 10, is of particular interest.

[33]C. T. Corcoran and P. W. Langhoff, Chem. Phys. Lett. (to be published).

[34]Results obtained for molecular systems are reported separately by P. W. Langhoff, S. R. Langhoff, and C. T. Corcoran (unpublished). We are informed that S. ONeil and W. P. Reindardt (unpublished) have recently completed a detailed study of the photoabsorption profile in molecular hydrogen, including treatment of the vibrational degree of freedom, employing the various procedures mentioned in Refs. 6 and 7.